

# The crystal structures of two lanthanide phosphites and the geometry of metal phosphite complexes

YiPing Zhang, Hengliang Hu and Abraham Clearfield\*

Department of Chemistry, Texas A&M University, College Station, TX 77843-3255 (USA)

(Received July 24, 1991; revised October 29, 1991)

## Abstract

As part of a continuing study on the synthesis and structure of metal phosphites, two compounds,  $\text{Ce}(\text{HO}_3\text{PH})(\text{O}_3\text{PH}) \cdot 2\text{H}_2\text{O}$  and  $\text{La}(\text{HO}_3\text{PH})(\text{O}_3\text{PH}) \cdot 3\text{H}_2\text{O}$  were prepared and their crystal structures determined by X-ray single crystal methods. The cerium compound crystallizes in the orthorhombic space group  $P2_12_12_1$  with  $a = 7.126(4)$ ,  $b = 16.539(4)$ ,  $c = 6.762(1)$  Å and  $Z = 4$ . The compound is a layered one with layers centered at  $\frac{1}{4}$  and  $\frac{3}{4}b$ . Each Ce is eight coordinate in a distorted dodecahedral geometry. One phosphite group chelates the metal and the chelating oxygens also bond to adjacent cerium atoms forming a chain. The other oxygen of this group bridges cerium atoms in a direction roughly perpendicular to the chain formed by the chelating oxygens to bind the chains into layers. The other phosphite group bridges adjacent cerium atoms along the same direction as the chelating atoms bridge and is alternately above and below the layer. The eighth coordination site is occupied by a water molecule. Another water molecule resides between the layers creating a hydrogen bond network which binds the layers together. The lanthanum compound is monoclinic,  $P2_1/c$  with  $a = 9.680(2)$ ,  $b = 7.135(1)$ ,  $c = 13.479(2)$  Å,  $\beta = 104.54(2)^\circ$ ,  $V = 901.0(3)$  Å<sup>3</sup> and  $Z = 4$ . The layer structure is very similar to that for the cerium phosphite but two water molecules reside between the layers binding them together through an extensive hydrogen-bond network. These structures are discussed in the light of previous work on phosphites and phosphonates.

## Introduction

In a recent publication [1] we described the structure of a new zinc phosphite of composition  $\text{Zn}(\text{HO}_3\text{PH})_2 \cdot 3\text{H}_2\text{O}$ . In this compound the structure is built up of Zn atoms coordinated to oxygen from six different phosphite groups. The octahedra are linked to  $\text{HPO}_2(\text{OH})$  tetrahedra via shared corners and also share edges to form infinite helical chains parallel to the  $c$  axis. The connectivity is such as to create large circular tunnels of about 6 Å diameter in the  $c$  axis direction. This phosphite forms double salts with alkali and alkaline earth ions [1, 2] that exhibit unusual structures. Therefore, we have undertaken to examine the preparation and structures of a variety of metal phosphites in the hopes of uncovering additional unusual structures. In this paper we describe the preparation and structure of two lanthanide phosphites.

Durand *et al.* [3] prepared all of the lanthanide phosphites of the type  $\text{Ln}(\text{HO}_3\text{PH})(\text{O}_3\text{PH}) \cdot 2\text{H}_2\text{O}$  and determined that they are orthorhombic with approximate cell dimensions of  $a = 16.5$ ,  $b = 7.1$  and  $c = 6.7$  Å. The thermal behavior of these compounds was also

examined and the phases formed by water loss identified. Subsequently they determined the structure of  $\text{Nd}(\text{HO}_3\text{PH})(\text{O}_3\text{PH}) \cdot 2\text{H}_2\text{O}$  [4]. The space group was found to be  $P2_12_12_1$  with  $a = 6.6840(9)$ ,  $b = 16.503(4)$  and  $c = 7.053(3)$  Å. However, they did not describe the structure as a layered one. It was therefore of interest to redetermine the structure of this class of compounds. We also prepared a trihydrate of lanthanum which will be described herein.

## Experimental

### Preparation of $\text{Ce}(\text{HO}_3\text{PH})(\text{O}_3\text{PH}) \cdot 2\text{H}_2\text{O}$

25 ml of a 1.0 M solution of  $\text{H}_3\text{PO}_3$  (Aldrich Chem.) were added to 30 ml of a 0.2 M solution of  $\text{Ce}(\text{NO}_3)_3 \cdot 6\text{H}_2\text{O}$  (Baker Reagent). The resulting colorless solution was kept in an oil bath at  $45 \pm 2$  °C for 10 days. As the volume of solution was reduced, large colorless needles formed at the bottom of the pyrex beaker. The crystals were recovered by filtration and washed with cold distilled, deionized water. The yield was about 30% but additional product could be obtained by continued evaporation of solvent.

\*Author to whom correspondence should be addressed.

*Preparation of La(HO<sub>3</sub>PH)(O<sub>3</sub>PH)·3H<sub>2</sub>O*

25 ml of an aqueous solution containing 0.5 M H<sub>3</sub>PO<sub>3</sub> and 0.5 M NaOH were added to a solution consisting of 1.86 g of LaCl<sub>3</sub>·7H<sub>2</sub>O (Baker Reagent) in 25 ml of distilled water. A white, gel-like precipitate formed. This gel was stirred overnight and then allowed to stand for one week during which time large, colorless needles formed.

*Instrumental*

Thermogravimetric analysis (TGA) was carried out with a duPont thermal analysis unit at a rate of 20°/min. IR spectra were obtained on a Digilab model FTS-40 FTIR unit by the KBr disk method.

*X-ray single crystal measurements*

All measurements were made on a Rigaku AFC5R diffractometer using an RU200 12-kW rotating-anode generator with graphite-monochromated Mo K $\alpha$  radiation ( $\lambda_{K\alpha} = 0.71069 \text{ \AA}$ ). Experimental conditions and crystallographic parameters for both compounds are presented in Table 1. In both cases, data were collected at ambient temperature. Crystals were mounted on glass fibers in a random orientation. The diameter of the incident beam collimator was 0.5 mm and the crystal to detector distance 22.5 cm. MSC/AFC control software [5] was used for the data collection.

Intensities were measured as  $C - \frac{1}{2}(t_c/t_b)(b_1 + b_2)$ , where  $C$  = total number of counts,  $t_c$  = time spent counting peak intensity,  $t_b$  = time spent counting one side of background,  $b_1$  = high-angle background counts,  $b_2$  = low-angle background counts; the intensity error  $\sigma(F^2) = [C + \frac{1}{4}(t_c/t_b)^2(b_1 + b_2) + PI]^2$ , where  $I$  intensity and  $P$  is the factor that downweights strong reflections,

equal in this case to 0.05. All calculations in the structure solution and refinement were made by using the TEXSAN crystallographic software package [6] on a MicroVAX-II-based system. Neutral-atom scattering factors were taken from Cromer and Waber [7]. Anomalous dispersion effects [8] were included in the calculation of  $F$  values using the anomalous dispersion terms  $\Delta f'$  and  $\Delta f''$  from the compilation due to Cromer [9].

*Ce(HO<sub>3</sub>PH)(O<sub>3</sub>PH)·2H<sub>2</sub>O*

Cell parameters and an orientation matrix for data collection were obtained from least-squares refinement of 25 accurately refined reflections in the angular range  $25^\circ < 2\theta < 35^\circ$ . Based on the systematic absences  $h00: h = 2n + 1; 0k0: k = 2n + 1; 00l: l = 2n + 1$  and the successful structure solution and refinement of the structure the space group was determined to be  $P2_12_12_1$  (No. 19). Data were collected in AUTO mode by using the  $\omega$ - $2\theta$  scan technique at a scan speed of 16°/min in  $\omega$ . The weak reflections ( $F < 10\sigma(F)$ ) were rescanned twice and the counts accumulated to assure good counting statistics. Stationary background counts were recorded on each side of the reflection with the ratio of peak counting time to background counting time equal to 2:1. A total of 867 reflections out to  $50^\circ$  in  $2\theta$  was collected of which 711 were greater than  $3\sigma(I)$ . The intensities of three representative reflections, that were measured after every 150 reflections, remained constant throughout data collection, indicating crystal and electronic stability. An empirical absorption correction, using program DIFABS [10], was applied and the data were corrected for Lorentz and polarization effects.

TABLE 1. Crystallographic data for lanthanide phosphites

Empirical formula	LaP <sub>2</sub> O <sub>9</sub> H <sub>9</sub>	CeP <sub>2</sub> O <sub>8</sub> H <sub>7</sub>
Formula weight	353.92	337.12
Crystal color, habit	colorless, needles	colorless needles
Crystal dimensions (mm)	0.17 × 0.05 × 0.02	0.03 × 0.04 × 0.2
Crystal system	monoclinic	orthorhombic
$a$ (Å)	9.680(2)	7.126(4)
$b$ (Å)	7.135(1)	16.539(4)
$c$ (Å)	13.479(2)	6.762(1)
$\beta$ (°)	104.54(2)	
$V$ (Å <sup>3</sup> )	901.0(3)	797.0(5)
Space group	$P2_1/c$ (No. 14)	$P2_12_12_1$ (No. 19)
$Z$ value	4	4
$D_c$ (g/cm <sup>3</sup> )	2.609	2.809
$F(000)$	672	636
$\mu$ (Mo K $\alpha$ ) (cm <sup>-1</sup> )	51.26	62.0
Radiation	Mo K $\alpha$ (=0.71069 Å)	Mo K $\alpha$
Temperature (°C)	23 ± 1	23 ± 1
Transmission coefficient	0.96–1.11	0.9–1.11
No. observations ( $I > 3\sigma(I)$ )	956	711
No. variables	109	101
Residuals: $R; R_w(F_o)$	0.032; 0.036	0.028, 0.034
Goodness of fit indicator, $S$	1.12	0.879

The structure was solved by direct methods [11a] followed by difference Fourier syntheses [11b]. The non-hydrogen atoms were refined with anisotropic thermal factors. The hydrogen atoms bonded to phosphorus were put in calculated positions. The final cycle of full-matrix least-squares refinement\* was based on 711 observed reflections  $I > 3\sigma(I)$  and 101 variable parameters with unweighted ( $R$ ) and weighted agreement factors ( $R_w$ ) as defined by  $R = \Sigma ||F_o| - |F_c|| / \Sigma |F_o|$ ;  $R_w = [\Sigma_w (|F_o| - |F_c|)^2]^{1/2}$ . Values of  $R = 0.032$  and  $R_w = 0.041$  were obtained. The maximum and minimum peaks on the final difference Fourier map corresponded to 0.90 and  $-0.91 e/\text{\AA}^3$ . The standard deviation on an observation of unit weight\*\* was 1.04. At this point a calculation of  $R$  and  $R_w$  was carried out with the signs of the  $F_c$  terms reversed to determine which is the correct enantiomorph. The new agreement factors were significantly lower as shown by the values given in Table 1.

### *La(HO<sub>3</sub>PH)(O<sub>3</sub>PH) · 3H<sub>2</sub>O*

The procedures used were very similar to those described above for the cerium compound. Cell parameters and an orientation matrix were obtained from a least-squares refinement of the setting angles of 25 reflections observed in the angular range  $34 < 2\theta < 40^\circ$ . Based on systematic absences of  $h0l: l = 2n + 1$ ,  $0k0: k = 2n + 1$  the space group was fixed as  $P2_1/c$  (No. 14). A total of 1858 reflections was measured at a speed of  $32^\circ/\text{min}$  (in omega) by the  $\omega$ - $2\theta$  method. Of these 1750 were unique. The intensities of three representative reflections were measured every 150 reflections and found to remain constant throughout data collection indicating crystal and electronic stability. The data were corrected for Lorentz and polarization effects and for absorption using program DIFABS [10].

This structure was also solved by direct methods and refined as described for the cerium phosphite. The final cycle of full-matrix least-squares refinement was based on 956 observed reflections with  $I > 3\sigma(I)$  and 109 variable parameters and converged (largest parameter shift was 0.02 times its e.s.d.) with unweighted and weighted agreement factors of  $R = 0.032$  and  $R_w = 0.036$ , respectively. Only the hydrogens bonded to phosphorus atoms were included in the refinement. The maximum and minimum peaks in the difference map were  $+0.77$  and  $-0.74 e/\text{\AA}^3$ , respectively.

\*The function minimized in the least-squares analysis was  $\Sigma_w (|F_o| - |F_c|)^2$ , where  $\omega = 4F_o^2/\sigma^2(F_o^2)$ ,  $\sigma^2(F_o^2) = [S^2(C + R^2B) + (PF_o^2)^2]/(Lp)^2$ ,  $s$  = scan rate,  $c$  = total integrated peak count,  $R$  = ratio of scan time to background counting time,  $B$  = total background count,  $Lp$  = Lorentz-polarization factor, and  $P$  =  $P$  factor.

\*\*The standard deviation of an observation of unit weight is expressed as  $[\Sigma_w (|F_o| - |F_c|)^2 (N_o - N_v)]^{1/2}$ , where  $N_o$  = no. of observations and  $N_v$  = no. of variables.

## Results

### *Ce(HO<sub>3</sub>PH)(O<sub>3</sub>PH) · 2H<sub>2</sub>O*

The final positional parameters together with isotropic temperature factors are given in Table 2. Bond distances and angles are given in Table 3. The structure is a layered one as seen most clearly in Fig. 1. The layers run parallel to the  $ac$  plane with their mean planes at  $b = \frac{1}{4}$  and  $\frac{3}{4}$ . Each Ce atom is eight coordinate as shown in Fig. 2, which also includes the numbering scheme for the atoms. Seven of the oxygens bonded to cerium originate from phosphite groups while the eighth is from a coordinated water molecule (O7). There are two types of phosphite groups in terms of their mode of coordination. The one containing P2 chelates the metal through oxygens O5 and O6, at the same time these oxygens bond to adjacent Ce atoms parallel to the  $a$  axis. The remaining oxygen, O4, then bridges to a Ce, connecting the rows along the  $c$  direction. This oxygen atom is two coordinate while those involved in chelation are three coordinate (Fig. 3). The second phosphite group bridges cerium atoms along the  $a$  direction through oxygens O1 and O2. This leaves O3 bonded only to P1 and therefore we assign the proton to it making it a P-OH group. The P<sub>1</sub>-O3 bond distance at 1.58(1) Å is significantly longer than the other P-O distances in this phosphite group. Cerium-oxygen bond distances range from 2.374(7) to 2.591(8) Å. However, the two longest bonds are formed by the chelating oxygens O5 and O6 while the shortest arises from the bridging phosphite oxygen O4. The remaining bridging oxygens and the water molecule all have approximately the same bond distance at 2.49(1) Å which is intermediate between the extremes. This arrangement produces a distorted dodecahedral coordination sphere, which is similar to those formed by layered rare earth phosphonates [12].

TABLE 2. Positional parameters and  $B_{eq}$  for  $Ce(HO_3PH)(O_3PH) \cdot 2H_2O$

Atom	$x$	$y$	$z$	$B_{eq}$ (Å <sup>2</sup> )
Ce(1)	0.4125(1)	0.78336(4)	0.1371(1)	0.73(2)
P(1)	0.2280(4)	0.5784(2)	0.1120(5)	1.3(1)
P(2)	0.4059(5)	0.7430(2)	0.6735(4)	1.0(1)
O(1)	0.392(1)	0.6333(5)	0.144(2)	2.1(4)
O(2)	0.120(1)	0.5962(6)	-0.075(1)	1.6(4)
O(3)	0.296(1)	0.4875(5)	0.100(2)	2.5(5)
O(4)	0.414(1)	0.7944(5)	0.487(1)	1.4(3)
O(5)	0.236(1)	0.7645(5)	0.805(1)	1.1(3)
O(6)	0.576(1)	0.7519(5)	0.808(1)	1.3(3)
O(7)	0.222(1)	0.9097(6)	0.121(2)	4.0(6)
O(8)	0.174(2)	0.9369(7)	0.594(2)	4.5(6)
H(1)	0.0986	0.5705	0.2602	4.0
H(2)	0.4035	0.6665	0.5963	4.0

TABLE 3. Intramolecular bond distances (Å) and angles (°) for  $\text{Ce}(\text{HO}_3\text{PH})(\text{O}_3\text{PH}) \cdot 2\text{H}_2\text{O}$  (with e.s.d.s in the least significant figure in parentheses)

Bond distances			
Ce1–P2	3.205(3)	P1–O1	1.495(9)
Ce1–O1	2.486(8)	P1–O2	1.51(1)
Ce1–O2A <sup>a</sup>	2.515(9)	P1–O3	1.583(9)
Ce1–O4	2.374(7)	P1–H1	1.368
Ce1–O5A <sup>b</sup>	2.591(8)	P2–O4	1.521(8)
Ce1–O5B <sup>c</sup>	2.471(8)	P2–O5	1.541(9)
Ce1–O6B <sup>d</sup>	2.496(9)	P2–O6	1.523(9)
Ce1–O6A <sup>b</sup>	2.564(8)	P2–H2	1.369
Ce1–O7	2.492(9)		
Bond angles			
O1–Ce1–O2	145.9(3)	O5A–Ce1–O6A	56.2(2)
O1–Ce1–O4	93.4(3)	O5A–Ce1–O7	78.5(4)
O1–Ce1–O5A	82.3(3)	O5B–Ce1–O6B	143.1(3)
O1–Ce1–O5B	74.5(3)	O5B–Ce1–O6A	69.4(3)
O1–Ce1–O6B	73.0(3)	O5B–Ce1–O7	141.5(3)
O1–Ce1–O6A	80.8(3)	O6B–Ce1–O6A	121.2(2)
O1–Ce1–O7	143.6(3)	O6B–Ce1–O7	71.4(3)
O2A–Ce1–O4	95.9(3)	O6A–Ce1–O7	112.3(4)
O2A–Ce1–O5A	103.6(3)	O1–P1–O2	113.5(6)
O2A–Ce1–O5B	74.4(3)	O1–P1–O3	110.2(5)
O2A–Ce1–O6B	140.8(3)	O1–P1–H1	118.68
O2A–Ce1–O6A	75.5(3)	O2–P1–O3	107.5(6)
O2A–Ce1–O7	69.4(3)	O2–P1–H1	106.80
O4–Ce1–O5A	151.0(3)	O3–P1–H1	98.81
O4–Ce1–O5B	82.2(3)	O4–P2–O5	112.2(5)
O4–Ce1–O6B	82.7(3)	O4–P2–O6	114.4(5)
O4–Ce1–O6A	151.5(3)	O4–P2–H2	101.57
O4–Ce1–O7	88.9(4)	O5–P2–O6	104.8(4)
O5A–Ce1–O5B	123.4(2)	O5–P2–H2	115.04
O5A–Ce1–O6B	68.6(2)	O6–P2–H2	109.09

<sup>a</sup>In symmetry position  $\frac{1}{2}+x, \frac{3}{2}-y, -z$ . <sup>b</sup>In symmetry position  $x, y, z-1$ . <sup>c</sup>In symmetry position  $\frac{1}{2}+x, \frac{3}{2}-y, 1-z$ . <sup>d</sup>In symmetry position  $x-\frac{1}{2}, \frac{3}{2}-y, 1-z$ .

The second water molecule (O8) resides between the layers as seen in Figs. 1 and 3 and is 2.65(1) Å from the coordinated water molecule. O8 is 3.00(1) Å from O4 and 2.92(2) Å from O1. Thus, O8 must be the donor in forming weak hydrogen bonds with these atoms and in turn act as the acceptor in the strong hydrogen bond to the coordinated water molecule. This latter water also acts as donor forming another hydrogen bond with O2 equal to 2.85(1) Å in O–O distance. These hydrogen bonds bind the layers together through the presence of the uncoordinated water molecule while the layers are also connected through formation of a strong P–OH interlayer hydrogen bond to O2(O3–O2, 2.66(1) Å).

#### $\text{La}(\text{HO}_3\text{PH})(\text{O}_3\text{PH}) \cdot 3\text{H}_2\text{O}$

The final positional and isotropic thermal parameters are given in Table 4. The important interatomic distances are given in Table 5 while the bond angles are collected in Table 6. This structure is also a layered one with

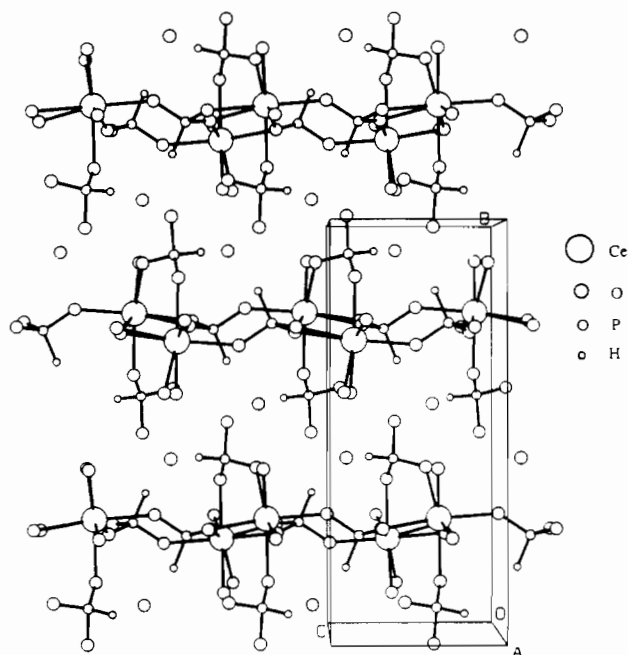


Fig. 1. Struplot representation of  $\text{Ce}(\text{HO}_3\text{PH})(\text{O}_3\text{PH}) \cdot 2\text{H}_2\text{O}$  as viewed down the  $a$  axis showing the layered nature of the compound. Note the zigzag nature of the layers parallel to the  $c$  axis direction.

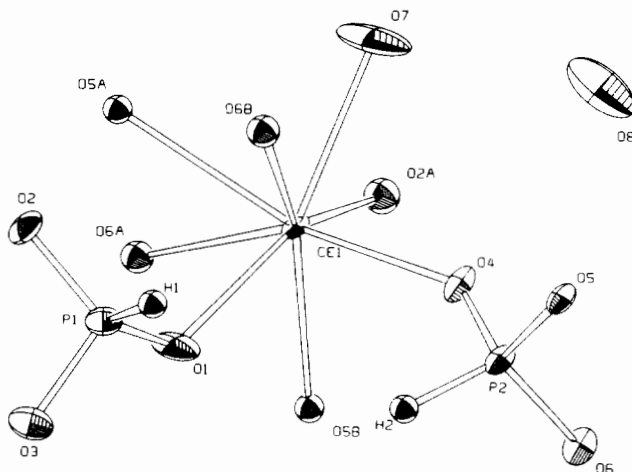


Fig. 2. An ORTEP drawing of a portion of the cerium phosphite structure showing the coordination about the Ce atom and the numbering scheme used in the tables. Thermal ellipsoids are at the 50% probability level. O7 represents the coordinated water oxygen and O8 is the oxygen atom of the water molecule which resides between the layers. Only the hydrogen atoms bonded to phosphorus are shown.

a layer structure similar to that of the cerium phosphite. Figure 4 shows the coordination about the lanthanum together with the atom numbering scheme. It is seen that lanthanum is chelated by the P1 phosphite group by oxygen atoms O1 and O2. The La–O2 bond distance is significantly larger than the La–O1 bond, which tilts the phosphite group to accommodate O3 bonding to

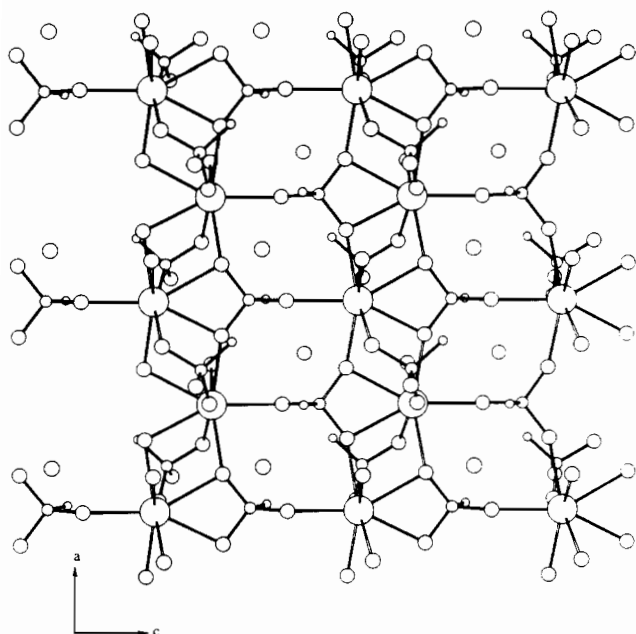


Fig. 3. A struplot representation of the layers in  $\text{Ce}(\text{HO}_3\text{PH})(\text{O}_3\text{PH}) \cdot 2\text{H}_2\text{O}$  viewed down the  $b$  axis. The layers are parallel to the  $ac$  plane.

TABLE 4. Positional parameters and  $B_{\text{eq}}$  for  $\text{La}(\text{HO}_3\text{PH})(\text{O}_3\text{PH}) \cdot 3\text{H}_2\text{O}$

Atom	$x$	$y$	$z$	$B_{\text{eq}}$ ( $\text{\AA}^2$ )
La(1)	0.06830(7)	0.2379(1)	0.83113(4)	0.99(2)
P(1)	-0.0165(3)	0.2289(4)	0.5838(2)	1.2(1)
P(2)	-0.3018(3)	0.0654(4)	0.7666(3)	2.0(1)
O(1)	0.020(1)	0.065(1)	0.6597(6)	1.2(3)
O(2)	-0.016(1)	0.402(1)	0.6473(7)	1.5(3)
O(3)	0.0814(7)	0.233(1)	0.5123(5)	1.6(3)
O(4)	-0.1916(8)	0.218(1)	0.8041(6)	2.4(3)
O(5)	-0.447(1)	0.168(1)	0.7232(8)	3.9(4)
O(6)	-0.271(1)	0.068(1)	0.6892(7)	2.9(4)
O(7)	0.307(1)	0.083(1)	0.9083(8)	3.5(4)
O(8)	0.6822(9)	-0.010(1)	0.3774(7)	2.7(4)
O(9)	0.5666(9)	0.242(2)	0.5012(7)	4.1(4)
H(1)	-0.1525	0.2408	0.5224	4.0
H(2)	-0.3302	-0.0285	0.8482	4.0

an adjacent La atom parallel to the  $c$  axis direction. These bonds are also the longest ones in the La coordination sphere. O1 and O2 also donate electron pairs to adjacent La atoms running along the  $b$  axis direction and these bonds are somewhat shorter than the chelating ones. The remaining oxygen of this phosphite group, O3, bridges in an approximately perpendicular direction to the O1–O2 line. The second phosphite group, originating from P2, then bridges adjacent La atoms through O4 and O6. These bonds formed by O2A, O1A, O3A are the shortest ones, probably because they are not constrained by the geometrical requirements of the four-membered chelate ring.

TABLE 5. Interatomic distances ( $\text{\AA}$ ) for  $\text{La}(\text{HO}_3\text{PH})(\text{O}_3\text{PH}) \cdot 3\text{H}_2\text{O}$

La1–O1	2.557(8)	P1–O1	1.536(8)
La1–O1A	2.500(7) <sup>a</sup>	P1–O2	1.504(8)
La1–O2	2.676(9)	P1–O3	1.511(7)
La1–O2A	2.480(7) <sup>c</sup>	P1–H1	1.370
La1–O3	2.423(6) <sup>b</sup>	P2–O4	1.519(9)
La1–O4	2.454(7)	P2–O5	1.566(9)
La1–O6A	2.478(9) <sup>a</sup>	P2–O6	1.492(9)
La1–O7	2.535(9)	P2–H2	1.374

<sup>a</sup>Atom is in symmetry position  $-x, \frac{1}{2}+y, \frac{3}{2}-z$ . <sup>b</sup>Atom is in symmetry position  $x, \frac{1}{2}-y, \frac{1}{2}+z$ . <sup>c</sup>Atom is in symmetry position  $-x, y-\frac{1}{2}, \frac{3}{2}-z$ .

TABLE 6. Selected bond angles ( $^\circ$ ) for  $\text{La}(\text{HO}_3\text{PH})(\text{O}_3\text{PH}) \cdot 3\text{H}_2\text{O}$

O1–La1–O1A	120.5(2)	O2–La1–O3A	145.3(3)
O1–La1–O2	55.3(2)	O2–La1–O4	79.9(3)
O1–La1–O2A	69.1(2)	O2–La1–O6A	73.7(3)
O1–La1–O3A	154.6(3)	O2–La1–O7	127.3(3)
O1–La1–O4	83.7(3)	O2A–La1–O3A	85.7(3)
O1–La1–O6A	98.0(3)	O2A–La1–O4	74.4(3)
O1–La1–O7	95.7(3)	O2A–La1–O6A	138.1(3)
O1A–La1–O2	66.9(2)	O2A–La1–O7	73.8(3)
O1A–La1–O2A	144.4(2)	O3A–La1–O4	86.9(2)
O1A–La1–O3A	78.6(2)	O3A–La1–O6A	102.8(3)
O1A–La1–O4	73.1(3)	O3A–La1–O7	79.1(3)
O1A–La1–O6A	76.9(3)	O4–La1–O6A	146.0(3)
O1A–La1–O7	132.5(3)	O4–La1–O7	146.0(3)
O2–La1–O2A	120.5(2)	O6A–La1–O7	68.0(3)
O1–P1–O2	106.2(4)	O4–P2–O5	106.2(5)
O1–P1–O3	111.3(5)	O4–P2–O6	116.3(5)
O1–P1–H1	118.41	O4–P2–H2	110.33
O2–P1–O3	115.7(5)	O5–P2–O6	110.7(5)
O2–P1–H1	99.03	O5–P2–H2	100.69
O3–P1–H1	105.97	O6–P2–H2	111.34

The coordination sphere is completed by a coordinative bonding of a water molecule, O7, to create the layers shown in Fig. 5. O5 is bonded only to P2 and therefore must also be bonded to a proton. Two water molecules reside between the layers as shown in Fig. 6. The layers are 9.37  $\text{\AA}$  apart which is 1.1  $\text{\AA}$  larger than the interlayer distance in  $\text{Ce}(\text{HO}_3\text{PH})(\text{O}_3\text{PH}) \cdot 2\text{H}_2\text{O}$ .

Table 7 lists the short interatomic O–O distances indicative of hydrogen bonding. The acid phosphite group binds a water molecule through a short hydrogen bond O5–H $\cdots$ O8 (2.59  $\text{\AA}$ ). In this case O5 is the donor because O8 in turn hydrogen bonds to O4 (2.72  $\text{\AA}$ ) and O3 (2.88  $\text{\AA}$ ). The coordinatively bound water O7 acts as donor to two water molecules represented by O9 in symmetry position 4 (2.81  $\text{\AA}$ ) and symmetry position 2 (2.86  $\text{\AA}$ ). O9 in turn acts as donor to O8 (2.86  $\text{\AA}$ ). The entire H-bond scheme ties the layers together as shown in Fig. 6.

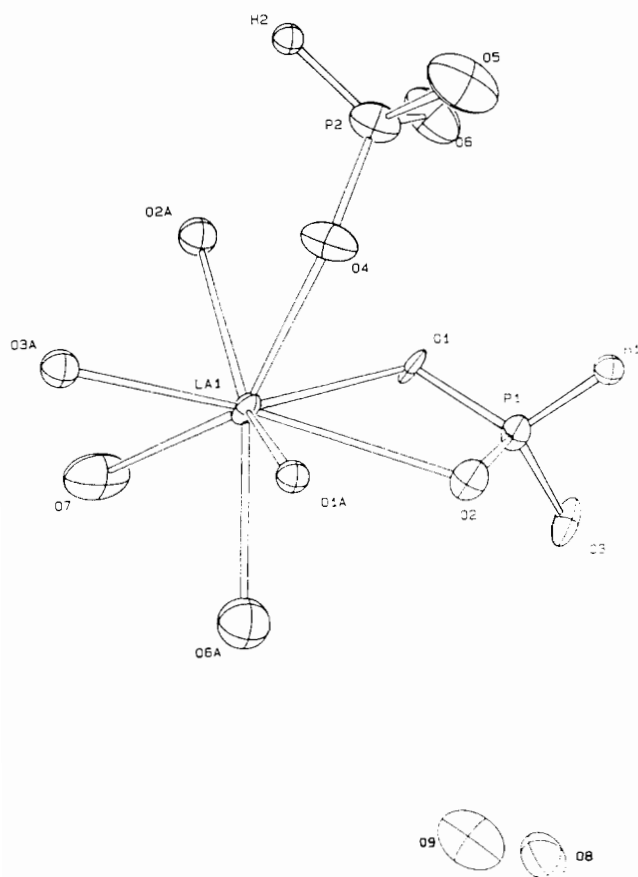


Fig. 4. ORTEP drawing of a portion of the  $\text{La}(\text{HO}_3\text{PH})(\text{O}_3\text{PH})\cdot 3\text{H}_2\text{O}$  structure showing the coordination about the La atom and the numbering scheme used in the tables. The thermal ellipsoids are at the 50% probability level. O7 represents the coordinated water oxygen and O8 and O9 are the oxygen atoms of the water molecules which reside between the layers. Only the hydrogen atoms bonded to phosphorus are shown.

## Discussion

The structure reported by Loukili *et al.* [4] for  $\text{Nd}(\text{HO}_3\text{PH})(\text{O}_3\text{PH})\cdot 2\text{H}_2\text{O}$  is essentially the same as that reported for the cerium compound in this work except for the choice of origin. However, they did not describe their structure as a layered compound. Furthermore, the hydrogen-bond scheme proposed by them differs from ours. These authors proposed four hydrogen bonds for the coordinated water molecule O7 (W1 in their notation) [4]. This would require the water oxygen to be five coordinate, an unlikely event. Also, the PO–H group forms a strong H bond to O2 (2.66 Å) in the next layer. Loukili *et al.* [4] gave a value of 2.87 Å for this bond. The scheme we have presented also binds the layers together through H bonding of the coordinated water to the interlamellar water which in turn H bonds to the framework oxygens of the adjacent layer. There

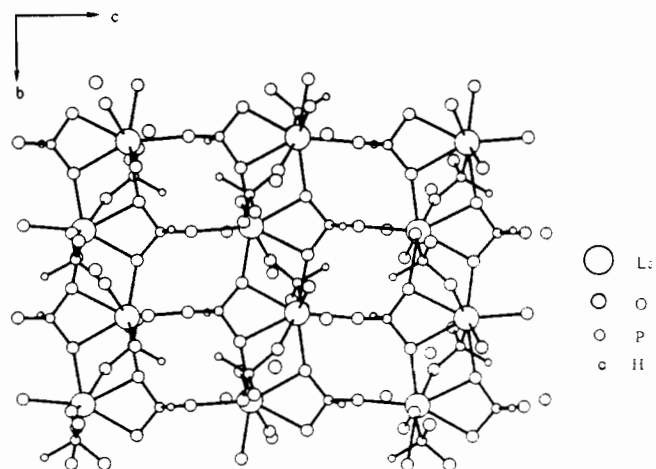


Fig. 5. A struplot representation of the  $\text{La}(\text{HO}_3\text{PH})(\text{O}_3\text{PH})\cdot 3\text{H}_2\text{O}$  layer as viewed down the  $a$  axis. The layers are parallel to the  $bc$  plane. Note the similarity to the layers in cerium phosphite, Fig. 3.

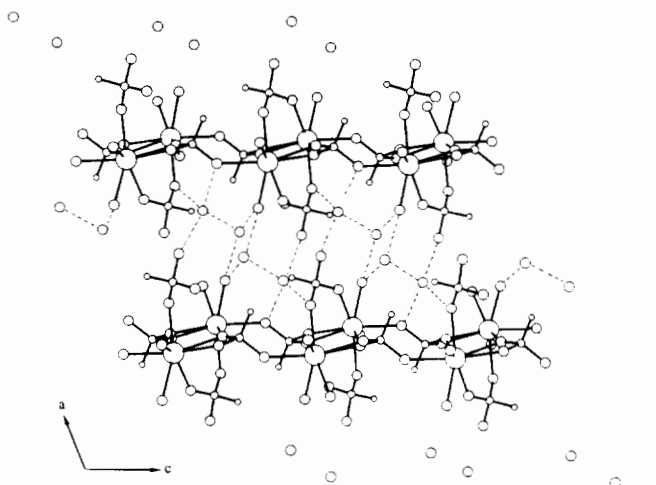


Fig. 6. A struplot representation of the lanthanum phosphite trihydrate structure as viewed down the  $b$  axis. Dashed lines indicate probable hydrogen bonds.

TABLE 7. Oxygen–oxygen interatomic distance (Å) denoting possible hydrogen bonding in  $\text{La}(\text{HO}_3\text{PH})(\text{O}_3\text{PH})\cdot 3\text{H}_2\text{O}$

O3–O8 <sup>a</sup>	2.88(1)	O7–O9 <sup>d</sup>	2.81(1)
O4–O8 <sup>b</sup>	2.72(1)	O7–O9 <sup>c</sup>	2.86(1)
O5–O8 <sup>c</sup>	2.59(1)	O8–O9	2.86(1)

<sup>a</sup>Symmetry code  $1-x, -y, 1-z$ . <sup>b</sup>Symmetry code  $x-1, \frac{1}{2}-y, \frac{1}{2}+z$ . <sup>c</sup>Symmetry code  $-x, -y, 1-z$ . <sup>d</sup>Symmetry code  $x, \frac{1}{2}-y, \frac{1}{2}+z$ . <sup>e</sup>Symmetry code  $1-x, y-\frac{1}{2}, \frac{1}{2}-z$ .

are no distinct  $[\text{H}_3\text{P}_2\text{O}_6]^{3-}$  anions in the structure as claimed [4]. Rather each phosphite group bonds to Ln through either chelation and bridging (one oxygen bridging 2 Ce) or by O–P–O bridges joining the metals

into layers. The hydrogen-bonding scheme binds the layers together in a natural way.

On heating one would expect the interlamellar water to be lost first, followed by the coordinated water. Reference to Fig. 1 shows that a small shift of the layers parallel to the *c* axis or in the *ac* plane would bring the P–OH groups from one layer close in to one in the adjacent layer allowing easy condensation of water to create pyrophosphite groups as reported from thermal studies [3].

At the time we were writing this manuscript the results of a study [13] on  $\text{La}(\text{HO}_3\text{PH})(\text{O}_3\text{PH}) \cdot 3\text{H}_2\text{O}$  appeared. Again the structure was described in terms which did not clearly indicate the layered nature of the compound. Also, the authors proposed that seven hydrogen bonds form based on O–O distances whereas we show six. They designated the seventh H bond as W3–O11, 2.82 Å or in our notation O7---O6. O7 is the coordinated water molecule which we have seen already acts as donor to two water molecules. In order to hydrogen bond with O6 the O7–H---O6 angle would be acute, which is unlikely.

Because of the foregoing incomplete structure descriptions in the literature we decided to examine some of the other reported phosphite structures. In the case of  $\text{Fe}(\text{HO}_3\text{PH})_3$  [14] and  $\text{La}(\text{HO}_3\text{PH})_3 \cdot \text{H}_2\text{O}$  [15] the authors propose that three hydrogen phosphite anions are hydrogen bonded together to constitute an  $(\text{HO}_3\text{PH})_3^{3-}$  anion. In point of fact, these compounds are layered as is clearly seen for the iron compound in Fig. 7. The Fe–O<sub>6</sub> octahedra are formed from six oxygens of six different phosphite groups all of which bridge two metal atoms. One third of the hydrogen bonds are within the layer and two thirds are between layers. There is no special phosphite anion.

In the case of  $\text{Cd}(\text{HO}_3\text{PH})_2 \cdot \text{H}_2\text{O}$  [16] linear chains parallel to the *b* axis direction are formed Fig. 8. Each Cd is six coordinate in which two types of phosphite

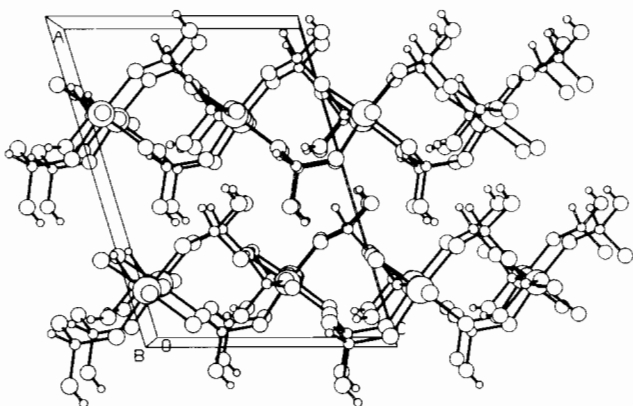


Fig. 7. A struplot representation of the  $\text{Fe}(\text{HO}_3\text{PH})_3$  structure as viewed down the *b* axis showing the layered nature of the compound.

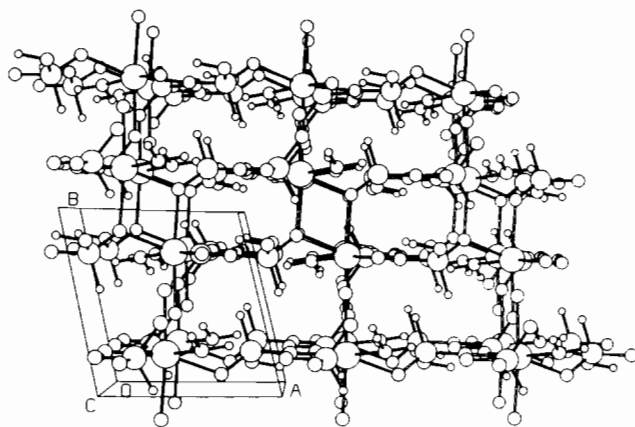


Fig. 8. A struplot representation of  $\text{Cd}(\text{HO}_3\text{PH})_2 \cdot \text{H}_2\text{O}$  showing the double bridged chains and the two types of phosphite bridging of Cd atoms.

bridging is observed. In the first there are double Cd–O–P–O–Cd type bridges, but they alternate with units of two cadmium atoms bridged (doubly) by a single oxygen from two phosphite groups. The hydrogen bonds O1–H4---O5 and O7–H2---O2 are between chains and do not indicate the formation of a special anion  $[\text{H}_4\text{P}_2\text{O}_6]^{2-}$  such as proposed [16].

Sufficient structures of both phosphites and phosphonates have now been completed so that some interesting comparisons can be made. In the lanthanum benzylphosphonate,  $\text{La}(\text{HO}_3\text{PCH}_2\text{C}_6\text{H}_5)(\text{O}_3\text{PCH}_2\text{C}_6\text{H}_5) \cdot 2\text{H}_2\text{O}$ , the La atom is eight coordinate [12], as it is in the phosphite. However, the bonding is slightly different. One of the phosphonate groups chelates the lanthanum atom but only one of these chelating oxygens bridges to an adjacent La. This failure of the other oxygen to bridge results from a tilting of the four-membered chelate ring to accommodate to the steric requirements of the benzyl group. The other phosphonate group, which contains a P–OH group, bridges lanthanum atoms in much the same way as the protonated phosphite group in  $\text{LaH}(\text{O}_3\text{PH})_2 \cdot 3\text{H}_2\text{O}$ . The third oxygen of the chelating phosphonate then links the chains into layers. In order to fill out the coordination sphere of La in the benzylphosphonate two water molecules coordinate to it.

In the zinc phenylphosphonate,  $\text{Zn}(\text{O}_3\text{PC}_6\text{H}_5) \cdot \text{H}_2\text{O}$  [17], and the divalent phosphonates in general [18] the metal is six coordinate. The phosphonate group chelates the metal and then both chelating oxygens bridge to adjacent divalent metals. The third oxygen bridges in a direction nearly perpendicular to that of the chelate oxygen bridges, creating layers much the same as described in this paper. The sixth coordination position is occupied by a water molecule. However, in phosphites, when all the phosphite groups are protonated, chelation does not take place and different structures result. In

$Zn(HO_3PH)_2 \cdot 3H_2O$  the Zn atom is octahedrally coordinated to oxygen atoms from six different phosphite groups all of which are bridging [1]. Thus, the octahedra share corners with the phosphite tetrahedra as stated in the 'Introduction'. A similar situation holds for  $Fe(HO_3PH)_3$  and  $Cd(HO_3PH)_2 \cdot H_2O$ . A second zinc phosphite,  $Zn_2(HPO_3)_2(H_2O)_4 \cdot H_2O$ , which was prepared under less acidic conditions, contained Zn atoms in both octahedral and tetrahedral coordination. All the phosphite groups bridged metal atoms so that no chelation type bonding was present. This arrangement led to a three dimensional structure with channels parallel to the *b* axis [1].

### Acknowledgement

This research was supported by the Robert A. Welch Foundation Grant No. A-673 for which grateful acknowledgement is made.

### References

- 1 C. Y. Ortiz-Avila, P. J. Squattrito, M. Shieh and A. Clearfield, *Inorg. Chem.*, **28** (1989) 2608.
- 2 M. Shieh, K. J. Martin, P. J. Squattrito and A. Clearfield, *Inorg. Chem.*, **29** (1990) 958.
- 3 J. Durand, M. Loukili, N. Tigani, M. Rafiq and L. Cot, *Eur. J. Solid State Inorg. Chem.*, **25** (1988) 297.
- 4 M. Loukili, J. Durand, L. Cot and M. Rafiq, *Acta Crystallogr., Sect. C*, **44** (1988) 6.
- 5 *CONTROL*, automation for Rigaku single crystal diffractometers, Molecular Structure Corp., College Station, TX, 1986 (revised 1988).
- 6 *TEXSAN*, structure analysis package, Molecular Structure Corp., College Station, TX, 1985 (revised 1988).
- 7 D. T. Cromer and J. T. Waber, *International Tables for X-ray Crystallography*, Vol. IV, Kynoch, Birmingham, UK, 1974, Table 2.2A.
- 8 J. A. Ibers and W. C. Hamilton, *Acta Crystallogr.*, **17** (1964) 781.
- 9 D. T. Cromer, *International Tables for X-ray Crystallography*, Vol. IV, Kynoch, Birmingham, UK, 1974, Table 2.3.1.
- 10 N. Walker and D. Stuart, *Acta Crystallogr., Sect. A*, **39** (1983) 158.
- 11 (a) C. J. Gilmore, *MITHRIL*, a computer program for the automatic solution of crystal structures from X-ray data, University of Glasgow, Glasgow, UK, 1983; (b) P. T. Beurskens, *DIRDIF; Direct Methods for Difference Structures*, an automatic procedure for phase extension and refinement of difference structure factors, *Tech. Rep. 1984/1*, Crystallographical Laboratory, Toernooiveld, 6526 ED Nijmegen, Netherlands, 1984.
- 12 R. C. Wang, Y. P. Zhang, P. J. Squattrito, H. Hu, R. Frausto and A. Clearfield, *Chem. Mater.*, submitted for publication.
- 13 M. Loukili, J. Durand, A. Larbet, L. Cot and M. Rafiq, *Acta Crystallogr., Sect. C*, **47** (1991) 477.
- 14 M. Sghyar, J. Durand, L. Cot and M. Rafiq, *Acta Crystallogr., Sect. C*, **47** (1991) 8.
- 15 P. N. Tuani, J. Durand and L. Cot, *Acta Crystallogr., Sect. C*, **44** (1988) 2048.
- 16 J. Loub, J. Podlahova and J. Jecny, *Acta Crystallogr., Sect. B*, **34** (1978) 32.
- 17 K. J. Martin, P. J. Squattrito and A. Clearfield, *Inorg. Chim. Acta*, **155** (1989) 7.
- 18 G. Cao, H. Lee, V. M. Lynch and T. E. Mallouk, *Inorg. Chem.*, **27** (1988) 2781.